



Article

Phytochemical-Assisted Fabrication of Biogenic Silver Nanoparticles from *Vitex negundo*: Structural Features, Antibacterial Activity, and Cytotoxicity Evaluation

Mohit Yadav ^{1,2}, Nisha Gaur ³, Nitin Wahi ⁴, Sandeep Singh ³, Krishan Kumar ⁵, Azadeh Amoozegar ⁶

- ¹ Jindal Global Business School, O.P. Jindal Global University, Sonipat 131001, India; mohitaug@gmail.com
- International School, Vietnam National University, Hanoi 11310, Vietnam
- ³ School of Biotechnology, Gautam Buddha University, Greater Noida 201312, India; gaurnisha2007@gmail.com (N.G.); sunnykumarsingh8163@gmail.com (S.S.)
- Department of Biotechnology, LNCT University, Kolar Road, Shirdipuram, Bhopal 462042, India; wahink@gmail.com
- Department of Chemistry, Indian Institute of Technology Delhi, Hauz Khas, New Delhi 110016, India; kjakhad21@gmail.com
- Faculty of Education and Liberal Arts, INTI International University, Persiaran Perdana BBN Putra Nilai, Nilai 71800, Negeri Sembilan, Malaysia; azadeh.amoozegar@newinti.edu.my
- * Correspondence: etibiotech@gmail.com

Abstract

Multidrug resistance (MDR) is an emerging global health concern worldwide, driving the need for innovative solutions. Herbal approaches are gaining attention and acceptance due to safer profiles and very few side effects. In this study, silver nanoparticles (VN-AgNPs) were synthesized using Vitex negundo, a medicinally valuable plant. A methanolic extract was prepared from Vitex negundo and the phytochemical evaluation confirmed the presence of flavonoids, alkaloids, and terpenoids, with quantitative analysis revealing high total phenolic content (TPC: 23.59 mg GAE/g) and total flavonoid content (TFC: 45.23 mg rutin/g), both maximized under microwave-assisted extraction (MAE). The antioxidant activity was also highest (18.77 mg AA/g). Characterization of the optimized extract by GC-MS identified various bioactive compounds. VN-AgNPs were synthesized using the aqueous leaf extract under specified conditions and were structurally characterized using many techniques and evaluated for antibacterial activity against four bacterial strains. VN-AgNPs exhibited significant antibacterial efficacy with inhibition zones measuring 16 ± 0.87 mm against Bacillus (Gram-positive), 15 ± 0.46 mm against E. coli (Gram-negative), 12 ± 0.64 mm against *Pseudomonas* (Gram-negative), and 11 ± 0.50 mm against *Pectobac*terium (Gram-negative plant pathogen). These findings highlight the efficacy of greensynthesized VN-AgNPs as a promising alternative to combat MDR pathogens, paving the way for sustainable and effective antimicrobial strategies.

Keywords: antibacterial; human health; bioactive phytochemicals; drug delivery; green synthesis of silver nanoparticles; MDR

check for **updates**

Academic Editors: Aleksandra Szcześ, Wuge Briscoe, Reinhard Miller, Milad Radiom and Anna Trybała

Received: 21 March 2025 Revised: 31 May 2025 Accepted: 12 June 2025 Published: 28 August 2025

Citation: Yadav, M.; Gaur, N.; Wahi, N.; Singh, S.; Kumar, K.; Amoozegar, A.; Sharma, E. Phytochemical-Assisted Fabrication of Biogenic Silver Nanoparticles from *Vitex negundo*: Structural Features, Antibacterial Activity, and Cytotoxicity Evaluation. *Colloids Interfaces* 2025, *9*, 55. https://doi.org/10.3390/colloids9050055

Copyright: © 2025 by the authors. Licensee MDPI, Basel, Switzerland. This article is an open access article distributed under the terms and conditions of the Creative Commons Attribution (CC BY) license (https://creativecommons.org/licenses/by/4.0/).

1. Introduction

Green synthesis of nanoparticles has become a widely adopted practice for sustainable application across different research fields. One such area is combating multidrug resistance (MDR) in microbes. Extracting of antimicrobial compounds from medicinaherbs,

combined with the application of nanotechnology, provides eco-friendly, economical, and safe alternatives to synthetic drugs [1,2]. Plants are particularly popular for eco-friendly synthesis of nanoparticles due to their abundance, accessibility, ease of handling, and rich phytochemical profile. These bioactive compounds act as capping and reducing agents in nanoparticle formation. Biologically synthesized nanoparticles are typically less toxic, more biocompatible, and more effective than their synthetic counterparts [3].

Vitex negundo, also known as Nirgundi (Family-Verbenaceae), contains a diverse range of secondary metabolites, such as iridoids, flavonoids, diterpenoids, phenols, and phytosterols [4]. These compounds contribute to extensive medicinal properties of the plant. Various species of Vitex negundo have shown analgesic, anti-inflammatory, antibacterial, antioxidant, and hepatoprotective effects [5]. However, its potential as a biogenic source for nanoparticle synthesis remains relatively underexplored. The use of medicinal plants in herbal formulation is an ancient global practice. The integration of these medicinal plants with nanotechnology opens new avenues for applications in medicine, agriculture, and environmental science [6]. Recent comparative studies on green-synthesized nanoparticles (GS-NPs) and chemically synthesized nanoparticles (CS-NPs) found that GS-NPs have superior antioxidative potential and lower cytotoxicity towards human tissues [7]. In terms of environmental impacts, cadmium oxide nanoparticles showed that GS-NPs were less toxic towards the environment as compared to CS-NPs [8]. GS-NPs offer a promising route for producing biocompatible and environmentally friendly nanomaterials with enhanced biological activities.

The quality of bioactive constituents plays a crucial role in enhancing the stability and efficacy of plant-derived nanoparticles. Among various extraction techniques, microwaveassisted extraction (MAE) is gaining attention due to its advantages—time efficiency, reduced solvent use, ease of handling, and cost-effectiveness—making it a preferable alternative to conventional methods [9]. Silver nanoparticles (AgNPs) exhibit potent antimicrobial properties against a wide range of pathogenic bacteria, fungi, and viruses. In some cases, their inhibitory effects surpass those of conventional antibiotics. Synthesizing AgNPs from plant extracts offers a promising strategy for treating MDR pathogens [10]. The antimicrobial potential of AgNPs depends upon various parameters such as size, shape, surface charges (zeta potential), colloidal states, and concentration. The key mechanism underlying the antimicrobial action of silver nanoparticles is that they attach to the cell surface of the pathogen, penetrate the microbial cell, generate reactive oxygen species (ROS), and disrupt the cell signaling pathway. However, AgNPs also exert toxic effects on human cells, depending on the cell type [11]. So, proper in silico analysis, in vivo testing, and controlled application are required when using silver nanoparticles for drug delivery systems. Identifying active compounds from plants, synthesizing eco-friendly nanoparticles, and evaluating their antibacterial properties offer numerous advantages and hold significant promise for advancing herbal drug discovery. This approach could support the development of novel antibacterial agents that serve as effective alternatives to synthetic drugs [12].

In this context, the present study aims to fabricate silver nanoparticles using aqueous leaf extract of *Vitex negundo*, thereby exploiting its intrinsic phytochemicals for reduction and stabilization. The synthesized nanoparticles were extensively characterized to determine their structural and morphological features using UV-Vis spectroscopy, FTIR, XRD, and electron microscopy techniques. Furthermore, their antibacterial efficacy against selected pathogenic strains was evaluated, along with preliminary cytotoxicity assessment to find their potential biomedical applicability. This study not only highlights the green synthesis of AgNPs using *Vitex negundo* but also explores their functionality as antimicrobial agents, thereby supporting the development of plant-based nanotherapeutics. Overall,

this study provides valuable insights for the design of safe and effective plant-based antibacterial agents.

2. Material and Methods

2.1. Plant Material

(*Vitex negundo*) was procured from CSIR-CIMAP, Lucknow, India, and cultivated in the herbal garden of Gautam Buddha University. Healthy, green, and fresh leaves of *Vitex negundo* were collected and rinsed under running tap water for 10 min. The leaves were then washed 2–3 times with double distilled water (DDW) and allowed to dry in the shade. Once fully dried, the leaves were ground into a fine powder and stored for further experiments.

2.2. Detection of Phytoconstituents

Vitex negundo leaf extract was prepared using methanol via three extraction methods: room temperature extraction (RTE), microwave-assisted extraction (MAE), and Soxhlet-assisted extraction (SAE). The leaf powder and methanol were used in a 1:20 (w/v) ratio.

For RTE, the mixture was placed in a shaking incubator at 120 RPM for 24 h at 37 $^{\circ}$ C. For MAE, the extraction was carried out under microwave conditions: 540 watts for 80 s. In the SAE method, the same ratio of leaf powder to methanol was used, but with a larger volume. The extraction was carried out using a Soxhlet apparatus (Sigma-Aldrich, Burlington, MA, USA) at 60 $^{\circ}$ C. After each extraction, the resulting mixture was centrifuged (Thermo Fisher, Powai, Mumbai, India) at $7000 \times g$ rpm for 8 min, and the supernatant was filtered. The filtered extract was stored at 4 $^{\circ}$ C for further analysis.

2.3. Bioactive Constituent Examination

2.3.1. Qualitative Screening

Initially, screening was performed to detect the presence of various phytochemicals, such as alkaloids, flavonoids, tannins, carbohydrates, and phenolic compounds. Qualitative phytochemical analysis was performed according to established methods of each test [13].

2.3.2. Quantitative Screening

Following the detection of the presence of various bioactive compounds in the leaf extract of *Vitex negundo*, their quantities were evaluated through specific assays. Total phenolic content (TPC) and total flavonoid content (TFC) and their total antioxidant capacity were analyzed as follows:

Total Phenol Content (TPC): TPC analysis was performed using the colorimetric method [13]. A standard curve was prepared using gallic acid at concentrations of 10, 20, 40, 80, and 100 μ g/mL. For each test, 50 μ L of various gallic acid concentrations and 500 μ L of distilled water were mixed with 100 μ L of Folin–Ciocalteu reagent. The mixture was incubated in the dark at room temperature for 5 min, followed by the addition of 300 μ L of 20% sodium carbonate. The reaction was allowed to proceed for 1 h at room temperature. Absorbance was measured at 750 nm. TPC was expressed as milligrams of gallic acid equivalents per gram of extract (mg GAE/g).

Total Flavanoid Content (TFC): Total flavonoid content was determined using the aluminum chloride colorimetric method [13]. A calibration curve was prepared using different concentrations of rutin (20, 40, 60, 80, 100, 120, 140, and 160 μ g/mL) from a stock solution of 1000 μ g/mL. For each assay, 0.5 mL of plant extract was mixed with 100 μ L of 20% AlCl₃ solution and incubated for 5 min. Then, 100 μ L of potassium acetate was added, followed by 5 mL of distilled water. The reaction was kept for 45 min in the dark,

Colloids Interfaces **2025**, 9, 55 4 of 20

and absorbance was taken at 415 nm. TFC was expressed as rutin equivalent per gram (mg of RE/g extract).

Total Antioxidant Capacity (TAC): Antioxidant capacity was determined using previously described method [14] with slight modifications. TAC was measured by a calibration curve using ascorbic acid (AA) at concentrations of 5, 10, 20, 30, 40, and 50 μ g/mL. For each test, 50 μ L of extract was mixed with 500 μ L of reagent solution (a mixture of 50 mL of concentrated 98% H₂SO₄, 0.2298 gm sodium phosphate, and 0.41 gm ammonium molybdate). The mixture was incubated at 90 °C for 45 min. The samples' absorbance was measured at 695 nm. TAC was calculated as the ascorbic acid equivalent per gram (mg of AA/g of extract).

2.3.3. GC-MS Chromatography

Vitex negundo leaf extract was subjected to GC-MS analysis using the Agilent 5977C GC/MSD system. Hydrogen gas was used as the carrier gas for the "Mass-Hunter OpenLab Data Acquisition B.08.01" CDS software platform, and the analysis was conducted on the "Mass Hunter with an open lab CDS". The ratio (m/z) ranges from 0.6 to 1091, and the scan speed was \leq 20,000 Da/s. The bioactive constituents in the leaf extract were confirmed by comparing their retention time (min), peak area, peak height, and mass spectral patterns to those in the "National Institute of Standards and Technology's (NIST)" spectral database of authentic compounds and other literature-based references [15,16].

2.4. Optimization of Bio Fabrication of VN-AgNPs

VN-AgNPs were formed by taking *Vitex negundo* leaf (20 g), and extract was prepared in 100 mL of distilled water by boiling the mixture at 60 °C for 60 min. The mixture was allowed to cool, and then filtered extract was used in the synthesis of silver nanoparticles by following the procedure: Leaf extract and AgNO₃ were mixed in a 1:5 ratio (v/v). The mixture was heated at 60 °C for 60 min. A color change from yellow to brown indicated the formation of nanoparticles. The mixture was then allowed to cool and centrifuged at $12,000 \times g$ rpm for 10 min to collect the nanoparticle. Pellets were washed with deionized water followed by centrifugation to remove soluble contaminants. The purified nanoparticles were subjected to various characterization techniques to understand their physiochemical properties.

The following parameters including $AgNO_3$ concentrations, incubation time, pH, volume ratio of leaf extract to $AgNO_3$, and temperature were optimized for efficient synthesis of silver nanoparticles. All the parameter ranges were selected on the basis of previous studies.

2.4.1. Temperature

VN-AgNPs were synthesized at different temperatures (20 $^{\circ}$ C, 30 $^{\circ}$ C, 40 $^{\circ}$ C, 50 $^{\circ}$ C, 60 $^{\circ}$ C, and 70 $^{\circ}$ C) to determine the optimal temperature for nanoparticle formation.

2.4.2. Incubation Time

To evaluate the effect of incubation time on the synthesis of VN-AgNPs, different time intervals were selected as 0, 15, 30, 45, 60, 75, and 90 min, followed by the same procedure for each interval.

2.4.3. Effect of pH

The influence of pH on nanoparticle formation was assessed by adjusting the pH to 3, 5, 7, 8, 9, and 11, while keeping the other parameters constant.

Colloids Interfaces **2025**, 9, 55 5 of 20

2.4.4. Leaf Extract Volume

Silver nanoparticles were prepared by using varying volumes of leaf extract (5, 10, 15, and 20 mL) while keeping the overall volume constant (30 mL). The other parameters were kept unchanged.

2.4.5. AgNO₃ Concentration

AgNPs were synthesized using different concentrations of AgNO₃ (2 mM, 3 mM, 4 mM, and 5 mM) with the same volume of plant extract and other parameters constant.

2.5. Characterization of VN-AgNPs

The preliminary confirmation of nanoparticle formation from *Vitex negundo* leaf extract was carried out by a UV-VIS spectrophotometer (Lambda 1050 Perkin Elmer, Waltham, MA, USA).

2.5.1. UV-VIS Spectroscopy

A spectral analysis was performed by generating spectra of the sample in the range of 300–700 nm (Lambda 1050 Perkin Elmer). The peak was determined at the 400–450 nm range to confirm the formation of nanoparticles [17]. After obtaining the peak at 400–450 range, the synthesized nanoparticles were subjected to various characterization techniques to analyze morphological and physiochemical properties of VN-AgNPs.

2.5.2. FTIR (Fourier Transform Infrared) Analysis

The functional active groups associated with VN- were identified by FTIR analysis. The purified nanoparticles were dried at 60 $^{\circ}$ C. These samples were mixed with potassium bromide (KBr) powder and analyzed using a PerkinElmer FTIR spectrophotometer. The FTIR spectra were recorded in the range of 4000–400 cm $^{-1}$ [18].

2.5.3. X-Ray Diffraction Analysis (XRD)

XRD analysis was performed to study the crystal structure, oxidation state, and atomic arrangement of silver nanoparticles. An "X-ray diffractometer" (Bruker D8 Advanced, Malvern Panalytical, Gurugram, Haryana, India) running at 30 kV and 100 mA was used. Cu K α radiation with a wavelength of 1.5406 Å in the 20 range of 20° to 80° was used to record the spectra. Analysis was performed by GSAS-II software [19].

2.5.4. SEM-EDX

The surface morphology and size of VN-AgNPs were detected using field emission scanning electron microscopy and energy-dispersive X-ray (EDX) spectroscopy. Images were captured using JEOL JSM-7800F Prime equipment (Jeol, Akishima, Japan) at 10 kV and a 5 mm working distance, utilizing a Schottky field electron source [20]. A thin film of VN-AgNPs was applied on a carbon-coated copper grid and allowed to stand for two minutes. The film was then air dried at room temperature before being subjected to the electron beam.

2.5.5. Dynamic Light Scattering (DLS) and Zeta Potential

The surface charge and particle size of synthesized VN-AgNPS were analyzed using zeta potential and DLS methods. The magnitude of zeta potential gives information about the state of the nanoparticle and long-term stability in colloidal solutions. The zeta potential, hydrodynamic size distribution, and polydispersity index (PDI) of the green-synthesized nanoparticles were measured using a Zetasizer (Malvern Panalytical, Nano-ZS90 Series, Worocestershire, United Kingdom (UK)) [21].

2.6. Antibacterial and Hemolytic Activity

The antibacterial efficacy of VN-AgNPs was assessed against four bacterial strains by evaluating the zone of inhibition and determining the minimum inhibitory concentration (MIC). Bacterial strains were procured from MTCC, Chandigarh (*Escherichia coli* MTCC443, *Bacillus sphaericus* MTCC7542, *Pseudomonas aeruginosa* MTCC 2474, and *Pectobacterium carotovorum* MTCC 1428). In an antibacterial assay, the concentration of each bacterial culture was calibrated to 10⁸ cells/mL using 0.5 McFarland standards.

2.6.1. Disk Diffusion Method

The surfaces of Mueller–Hinton agar plates were inoculated with 1000 μ L of the bacterial suspension (10⁸ CFU/mL). The inoculum was allowed to dry completely. Neomycin was used as the positive control, and 100% methanol served as the negative control. Wells were punched into the agar, and each was filled with 50 μ L, 70 μ L, 90 μ L, and 110 μ L of silver nanoparticle solution. After allowing the solutions to absorb, the plates were incubated at 37 °C for 12 h. The zones of inhibition were then measured to evaluate antibacterial activity [22].

2.6.2. Hemolytic Activity

The hemolytic activity of VN-AgNPS was evaluated against normal murine erythrocytes following the method in [23]. "Mouse blood (3 mL) was mixed with 1XPhosphate-Buffered Saline (PBS-5 mL.), and the resultant mixture was centrifuged at $3000\times g$ rpm for 5 min. The pellets were suspended in 5 mL of PBS; 180 μ L was aliquoted, and 20 μ L, 40 μ L, 60 μ L, and 80 μ L of VN-AgNPs were incorporated and dissolved in dimethyl sulfoxide (DMSO)". Triton-X served as the control for the comparison study. Following a 30 min incubation at 37 °C, the sample was centrifuged for 5 min at $13,000\times g$ rpm and then chilled. Free hemoglobin in the supernatant was quantified at 576 nm using a spectrophotometer. DMSO and 1% Triton-X were taken as the negative control and positive control, respectively. Hemolysis (%) was calculated using the formula:

$$\label{eq:absorbance} \begin{split} & \text{\%Hemolysis} = (A_t - A_n)/A_s \times 100 \\ & A_t = \text{Absorbance of test sample;} \\ & A_n = \text{Absorbance of negative control;} \\ & A_s = \text{Absorbance of positive control.} \end{split}$$

2.7. Statistical Analysis

The variability among several components was examined using one-way ANOVA (single-factor analysis of variance). All experiments were conducted in triplicate, and results are presented as mean \pm standard error SE.

3. Results

3.1. Phytochemical Extraction

The extraction method has a significant impact on the quality of the medicinal plant extract [24]. Therefore, selecting an appropriate method is essential for efficient extraction of phytoconstituents. In this study, three methods (RTE, MAE, and SAE) were applied to obtain the extract from Vitex negundo leaves. The comparison among these extraction methods was based on the TPC and TFC present in the extract.

3.2. Phytochemical Screening

3.2.1. Qualitative

The qualitative analysis revealed that Vitex negundo leaves possess several bioactive secondary metabolites. A series of biochemical tests confirmed the presence of phenol,

flavonoids, alkaloids, tannins, and terpenoids. However, saponins were absent in all cases, as shown in "Supplementary Materials". These preliminary findings confirm the presence of various secondary metabolites that likely contribute to the medicinal properties of the plant. The presence of these bioactive compounds supports the known antimicrobial, antioxidant, and therapeutic applications of Vitex negundo, as also reported in earlier studies [25–27] that show the antifungal and antibacterial activities of polyphenols against clinical isolates. Many plant extracts exhibit a wide range of antibacterial activity against Pseudomonas aeruginosa, Staphylococcus aureus, Streptococcus epidermidis, Klebsiella pneumoniae, *E. coli, Listeria monocytogenes, Acinetobacter* sp., *Proteus* sp., *Micrococcus* sp., and *Bacillus* sp. All these plants, rich in antimicrobial polyphenols, represent a promising and powerful source of highly effective novel antibacterial agents.

3.2.2. Quantitative

Quantitative phytochemical analysis is essential for evaluating the bioactive potential of plant extracts, particularly through the assessment of total phenolic content (TPC), total flavonoid content (TFC), and total antioxidant capacity (TAC). TPC, TFC, and TAC of *Vitex negundo* leaf extracts were measured and expressed as gallic acid equivalents (GAE), rutin equivalents, and ascorbic acid equivalents (AAE) per gram of extract, respectively. Among the methods tested, MAE yielded the highest TPC (23.59 \pm 0.002 mg GAE/g), followed by SAE (20.26 \pm 0.03 mg GAE/g) and RTE (18.26 \pm 0.013 mg GAE/g). Similarly, MAE also produced the highest TFC (45.23 \pm 0.01 mg rutin/g), compared to RTE (34.52 \pm 0.032 mg rutin/g) and SAE (30.50 \pm 0.01 mg rutin/g). In terms of antioxidant activity, MAE again demonstrated superior performance, with the highest TAC value of 18.77 \pm 0.008 mg AAE/g, as shown in Figure 1. These quantitative results validate the efficiency of the MAE method in extracting phytochemicals from *Vitex negundo* leaves [28].

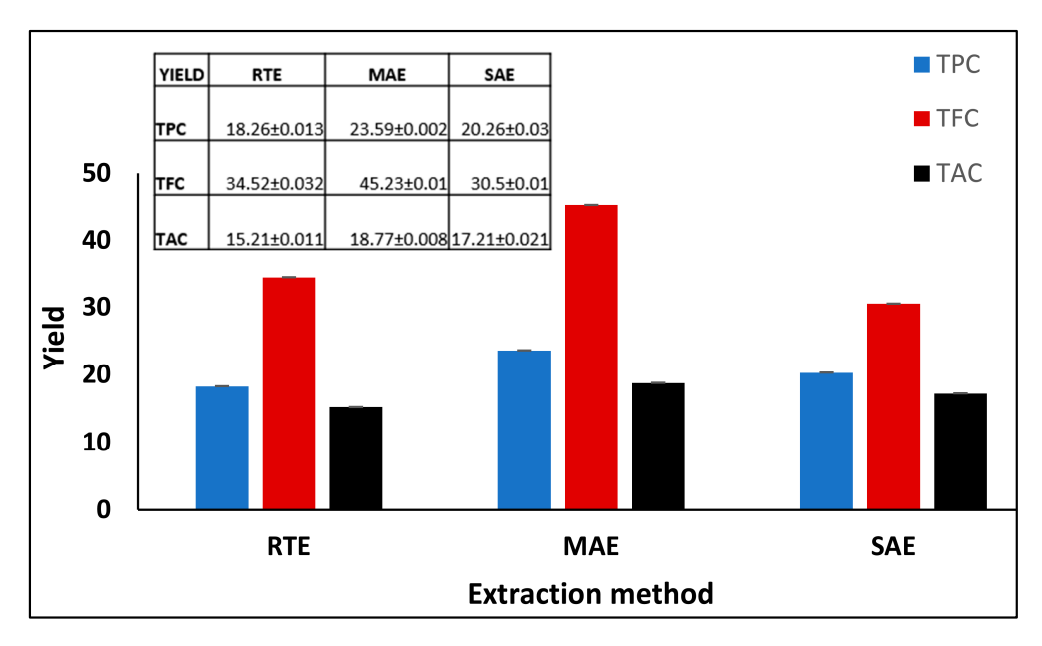


Figure 1. Comparative analysis of total phenolic content (TPC), total flavonoid content (TFC), and total antioxidant capacity (TAC) in *Vitex negundo* leaf extracts obtained using three extraction methods: room temperature extraction (RTE), microwave-assisted extraction (MAE), and Soxhlet-assisted extraction (SAE). Values are expressed as absorbance equivalents of gallic acid, rutin, and ascorbic acid, respectively. Error bars represent standard deviation from triplicate measurements.

3.2.3. GC-MS Chromatography

Vitex negundo leaf extract was subjected to GC-MS analysis to identify the bioactive compounds. Several compounds were identified in the extract, as shown in

"Supplementary Materials". The identification of compounds was based on retention time. The mass spectrum was interpreted using the NSIT database. The GC-MS chromatogram revealed nine peaks, each representing a distinct kind of bioactive component present in the extract. The major components were "3-ethenyldodecahydro-3,4a,7,7,10a-pentamethyl,2-propanon-1-hydroxyacetone, bis(2-methylpropyl) ester, 2,7-dioxatricyclo[4.4.0.0(3,8)]dec-4-ene,benzofuran, phenol, phen-1,4-diol, 2,3-dimethyl-5-trifluoromethyl, 1H-naphtho[2,1-b]pyran, -, [3R-(3 α ,4a β ,6a α ,10a β ,10b α)]-, 5-hydroxymethyl furfural, 1,2-benzenedicarboxylic acid, and 5-(7a-Isopropenyl-4,5-dimethyl-octahydroinden-4-yl)-3-methyl-pent-2-enal" [29].

These compounds have been previously reported as anti-inflammatory, antibacterial, and antioxidant in several medicinal plant studies. Phenolics, alkanes, aldehydes, esters, alkenes, and ketones are some examples of these substances. The antioxidant, antimicrobial, and anti-inflammatory properties of Vitex negundo leaf extract can be attributed to these bioactive compounds. It has been demonstrated that compound 1,2-benzene dicarboxylic acid possesses antioxidant, anti-inflammatory, and anti-cancer qualities. For bis (2-methylpropyl) ester of 1,2-benzene dicarboxylic acid (BDCe fraction) [30], human osteosarcoma MG-63, neuroblastoma IMR-32, and lung cancer A549 cell lines were used to assess the BDCe fraction's antiproliferative properties [31]. The anti-inflammatory qualities of 5-hydroxyfurfural(5-HMF) have also been studied in relation to lung conditions. The research indicated that 5-HMF decreased lipopolysaccharide (LPS)-induced ALI (acute lung injury) and had a protective impact on endotoxin-induced acute lung damage in mice via reducing alveolar destruction [32]. In another study, hydroxy furfural was isolated from Cola hispid and described as a possible lead for innovative medication development for the treatment of oral cancer and the suppression of a multidrug-resistant strain of S. aureus [33]. Various other medicinal plants with similar phytoconstituents have shown significant antibacterial, anti-inflammatory, and antioxidant effects [34]. The antioxidant potential is due to cyclic unsaturated chemicals [35,36].

3.3. Optimization of Bio Fabrication Process

Silver nanoparticles were successfully synthesized from the *Vitex negundo* leaf extract. The formation of VN-AgNPs was indicated by the color change from light yellow to dark brown. The color change occurs due to the molecular and structural rearrangements of molecules induced by the reducing agents present in the extract [37,38]. The synthesis is further confirmed by UV-visible spectroscopy that revealed a sharp peak at the range of 400–450 nm (Figure 2A). This observation is consistent with previous studies reporting that silver nanoparticle synthesis from many medicinal plants shows an absorption peak in the same range [39,40]. Silver nanoparticle synthesis is highly dependent on several key parameters that affect size, shape, morphology, and stability, such as AgNO₃ concentrations, time duration, pH of the medium ratio (v/v) leaf extract, and temperature [41]. All these parameters were systematically examined in this study to optimize the synthesis process and improve the quality of VN-AgNPs in terms of their size, shape, morphology, and stability.

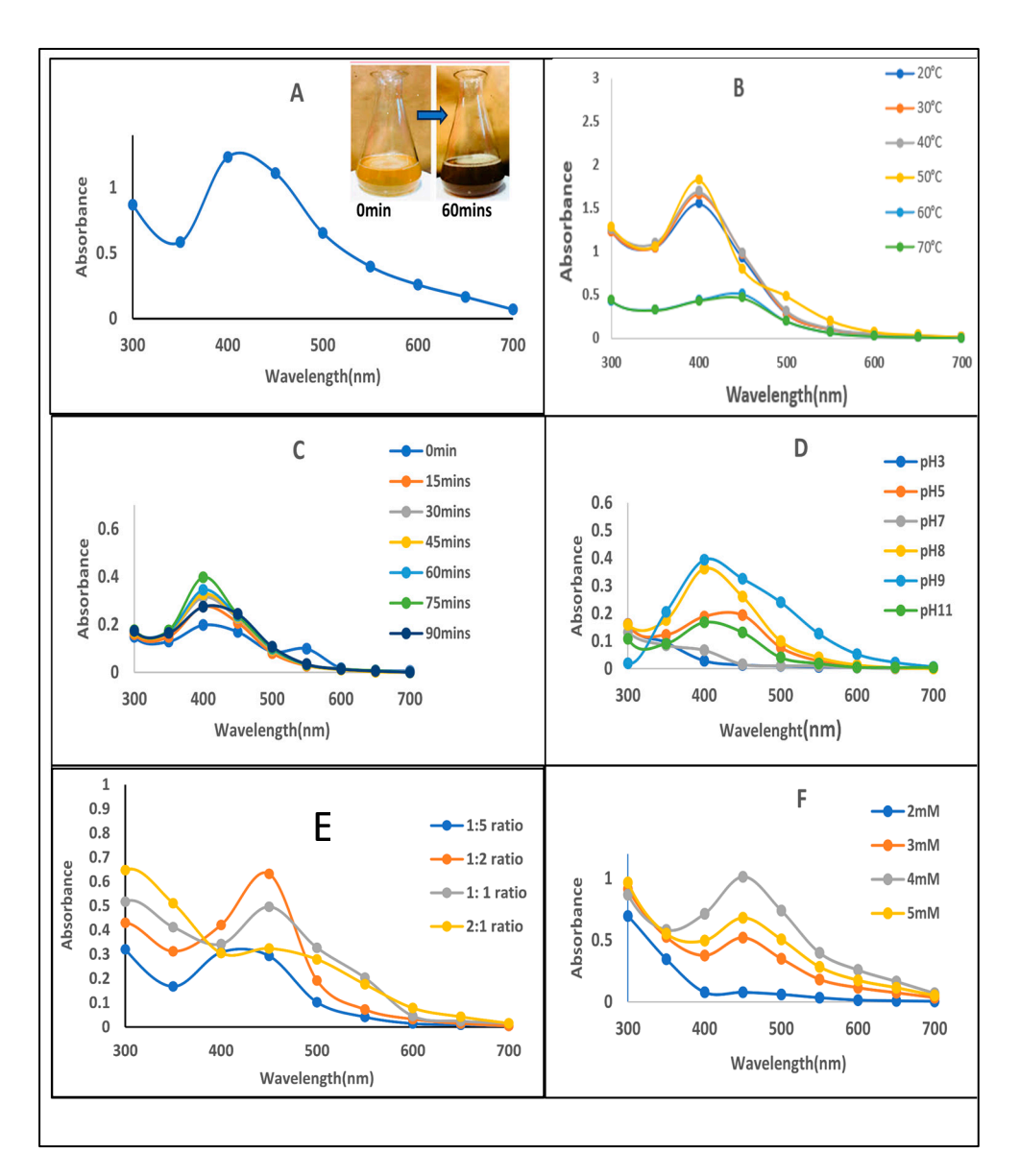


Figure 2. VN-AgNP synthesis and different parameter optimization. "(\mathbf{A})": UV spectra of synthesized nanoparticles at 300–700 nm with visible color change; "(\mathbf{B})": temperature effect; "(\mathbf{C})": time course; "(\mathbf{D})": pH optimization; "(\mathbf{E})": plant extract and silver nitrate ratio; "(\mathbf{F})": silver nitrate concentration.

3.3.1. Temperature Optima

The temperature course effect on VN-AgNP synthesis was also studied. All the samples were incubated at different temperatures (20, 30, 40, 50, 60 °C). It was observed that there was no significant change in the formation of nanoparticles in the range of 20 °C to 50 °C, as the peak was almost of similar absorbance. A further increase in temperature (60–70 °C) triggered the agglomeration and degradation in the reaction mixture and a decrease in absorption rate; therefore, 50 °C was selected for further experiment. This decline may be related to the formation of bigger particles and more aggregation at higher temperatures. At a lower temperature range, better nano-sizing may be due to less aggregation of developing AgNPs [42]. The optimal temperature of silver nanoparticle synthesis was 50 °C (Figure 2B). Similar results can be seen in another study that states the effect of temperature on silver nanoparticle synthesis [43], and the lower temperature favors the formation of nanoparticle formation in the solution.

3.3.2. Time Course

The effect of different time intervals (15, 30, 45, 60, 75, 90 min) was examined on nanoparticle formation. It was revealed that the rise in absorbance started at 30 min and continuously increased to 75 min. The highest absorbance was observed at 75 min (green line). When time increased further up to 90 min, a decrease in absorbance was observed. The increase in absorbance with time (up to 75 min) indicates progressive nanoparticle formation, followed by possible aggregation or stabilization at later time points (90 min). The UV-Vis spectra (Figure 2C) show a time-dependent increase in absorbance at ~400 nm, indicating the formation of silver nanoparticles via surface plasmon resonance (SPR). This trend is in line with earlier reports that observed similar SPR peaks in the 400–450 nm range for biologically synthesized AgNPs [44]. The decline in absorbance at 90 min suggests possible nanoparticle aggregation or saturation. No significant difference was observed between 60 and 75 min, so 60 min was taken as optimum for further experiments.

3.3.3. Effect of pH

The UV-Vis spectra indicated that acidic conditions (pH 3–5) were unfavorable for the synthesis of VN-AgNPs. Nanoparticle size is greatly influenced by the pH of the medium. In acidic conditions, the particle size is generally expected to be larger compared to basic conditions [45]. Observations revealed that an alkaline medium was more favorable, with increased absorbance at a basic pH of 8–9, as the spectra confirmed nanoparticle formation. However, a sharp decline in the peak was observed at pH 11 (Figure 2D). The most distinct and optimized peak was recorded at pH 9, which was subsequently used for further parameter optimization. This finding is consistent with results obtained using *Olea europaea* (olive) and *Ginkgo biloba* leaf extracts for silver nanoparticle synthesis, where an alkaline pH range of 9–11 was also found to be favorable [46,47].

3.3.4. Plant Extract Volume

To optimize the concentration ratio of leaf extract and silver nitrate for nanoparticle synthesis, various ratios were tested by adjusting the volumes of each component in a 30 mL reaction mixture. Leaf extract was added in volumes of 5, 10, 15, and 20 mL, while silver nitrate was added in corresponding volumes of 25, 20, 15, and 10 mL, resulting in ratios of 1:5, 1:2, 1:1, and 2:1, respectively. Maximum absorption was observed at a 1:2 ratio, with a characteristic peak at 430 nm (Figure 2E), indicating optimal nanoparticle synthesis. Lower (1:5) and higher ratios (1:1 and 2:1) were found to be less effective, as evidenced by reduced absorbance. These results align with those of previous studies, which reported that increasing plant extract concentration can lead to larger nanoparticle size and aggregation within the mixture [48].

3.3.5. Silver Nitrate Concentration

Silver nitrate concentration is a significant factor that influences the size and shape of synthesized silver nanoparticles. Various silver nitrate concentrations were tested to optimize AgNO₃ concentration. A shift in the absorption peak was noticed by changing AgNO₃ from 2 mM to 5 mM. The intensity of the peaks by UV spectra showed higher absorption at the 4 mM concentration, as shown in Figure 2F. The impact of silver nitrate on the shape and other characteristics of silver nanoparticles was also validated by another study cited in the literature. Silver nitrate (AgNO₃) concentration significantly impacts the synthesis of silver nanoparticles (AgNPs) from plants. Higher AgNO₃ concentrations generally lead to increased crystallite size and AgNP size. However, extremely high concentrations may not result in a significant increase in nanoparticle adsorption, potentially reaching an optimal

point. Furthermore, different concentrations can affect the color change, absorbance, and stability of the synthesized AgNPs [49].

After optimization of all the parameters, the yield of VN-AgNPs was also evaluated. The yield calculation was performed using an optimized protocol. A total of 20 g of fresh plant leaves was used to prepare 100 mL of aqueous leaf extract, which was then subjected to nanoparticle synthesis under optimized reaction conditions. Following the completion of the reaction and subsequent purification steps, the dried nanoparticle product was weighed. The final yield obtained was 0.234 g of dried nanoparticles. This corresponds to a nanoparticle yield of 1.17% (w/w) with respect to the initial plant biomass used. This quantitative assessment highlights the efficiency of the adopted green synthesis protocol and provides a basis for further scale-up and optimization studies.

3.4. Physiochemical Characteristics of VN-AgNPs

With the increasing use of nanoparticles in pharmaceutical applications, the characterization of synthesized silver nanoparticles is important. Nanoparticles possess a dynamic nature, so handling and processing are complex during the synthesis process. The physical and chemical properties have a significant influence on their systemic activities [50]. Therefore, characterization is necessary to find out the physiochemical properties of synthesized nanoparticles. Silver nanoparticles from *Vitex negundo* leaves were subjected to different techniques to determine the size, shape, surface morphology, and other characteristics.

3.4.1. UV-Visible Spectrophotometric Analysis

The optical features are used to access the size, shape, and distribution pattern of nanoparticles in the mixture. UV–visible spectroscopy is a kind of preliminary confirmation of the synthesis of nanoparticles [51]. The absorbance peak at 400–450 nm in the spectrum confirms the presence of silver nanoparticle synthesis, as shown in Figure 2A.

3.4.2. FTIR (Fourier Transform Infrared)

VN-AgNPs surface functional groups were identified by FTIR analysis. When nanoparticles were formed in the mixture, these functional groups served as stabilizing or capping agents. The FTIR spectrum displayed a number of absorption peaks. Peaks at 1029.3 cm⁻¹, 1066.96 cm⁻¹, 1378.46 cm⁻¹, and 1595.30 cm⁻¹ were measured. At 2920.44 cm⁻¹ and 3409.76 cm⁻¹, two more peaks were seen (Figure 3A). The spectrum is rich in oxygen- and nitrogen-containing functional groups, which are commonly found in plant extracts [52]. These groups are known to reduce metal ions and have a role in capping and stabilizing nanoparticles during synthesis. The peaks close to "1029.3 cm⁻¹ and 1066.96 cm⁻¹" were attributed to significant (C-O/C-N) stretching often seen in plant-derived capping agents. The (C-N) stretching and (C=C) stretching/N-H bending of amine's were represented by the peaks at 1378.46 cm⁻¹ and 1595.30 cm⁻¹, respectively. Two more peaks were identified as (O-H) stretching of alcohol and (N-H) stretching of aliphatic amine at 3409.76 cm⁻¹. The presence of an aliphatic chain indicated lipids or terpenoids possibly involved in nanoparticle stabilization.

The vitex leaf extract FTIR data ("Supplementary Materials") was also compared with the FTIR data of VN-AgNP formation, which clearly showed the shifting of peaks after nanoparticle formation. The shift in the hydroxyl (O-H), carbonyl (C=O), and C-O peaks suggests that phenolics, flavonoids or proteins in plant extracts are likely involved in reducing metal ions and stabilizing the nanoparticles. The disappearance of some peaks such as 2075 and 638 cm⁻¹ supports the chemical modification of these groups during synthesis. New bonding interactions may cause slight shifting and broadening of peaks. The obtained result is consistent with other research findings on *phylanthus acidus* [52] and Utrica dioica [53], which revealed the presence of various functional groups, including

aromatic rings, alkenes, alcohols, ethers, carboxylic acids, esters, nitro compounds, and hydrogen-bonded alcohols and phenols showing almost similar peaks in FTIR data, which confirms that common groups are involved in plant-mediated silver nanoparticle synthesis.

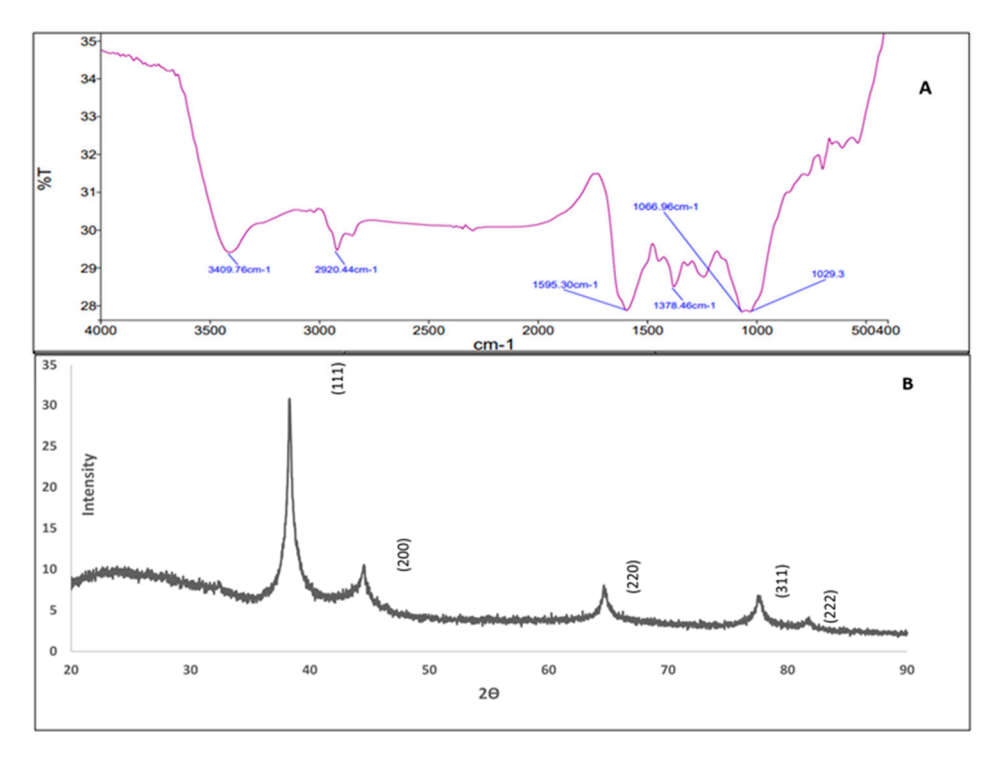


Figure 3. Characterization of VN-AgNPs: (A) FTIR spectra; (B) XRD spectra.

3.4.3. X-Ray Diffraction (XRD)

XRD analysis is another popular approach for characterizing green-produced NPs. It is used to determine the crystallinity of produced nanoparticles. The XRD peaks reveal whether the produced nanoparticles are crystalline or amorphous. It was utilized to investigate the atoms' spatial organization, overall oxidation status, and crystal structure of silver nanoparticles. The XRD spectra in Figure 3B demonstrate the existence of peaks at 20 values of 38.03°, 44.09°, 67.34°, 78.29°, and 82.03°, which correspond to the (211), (111), (220), (311), and (222) planes of silver. Thus, the XRD spectrum validated the silver nanoparticles' crystalline structure. Impurity peaks were not observed in the spectra, and the XRD pattern peaks may be easily attributed to a face-centered cubic structure of silver. These kinds of peaks were also observed in the previous studies [54,55] on silver nanoparticles.

3.4.4. SEM-EDX

Scanning electron microscopy (SEM) combined with energy-dispersive X-ray spectroscopy (EDX) is a widely used technique for characterizing silver nanoparticles (AgNPs). In this study, SEM-EDX analysis was conducted to examine the morphological and compositional properties of VN-AgNPs at the submicron scale. Field emission scanning electron microscopy (FESEM) revealed that the VN-AgNPs exhibited irregular granulated structures, including spherical and ellipsoidal shapes with smooth surfaces, as shown in Figure 4A,B.

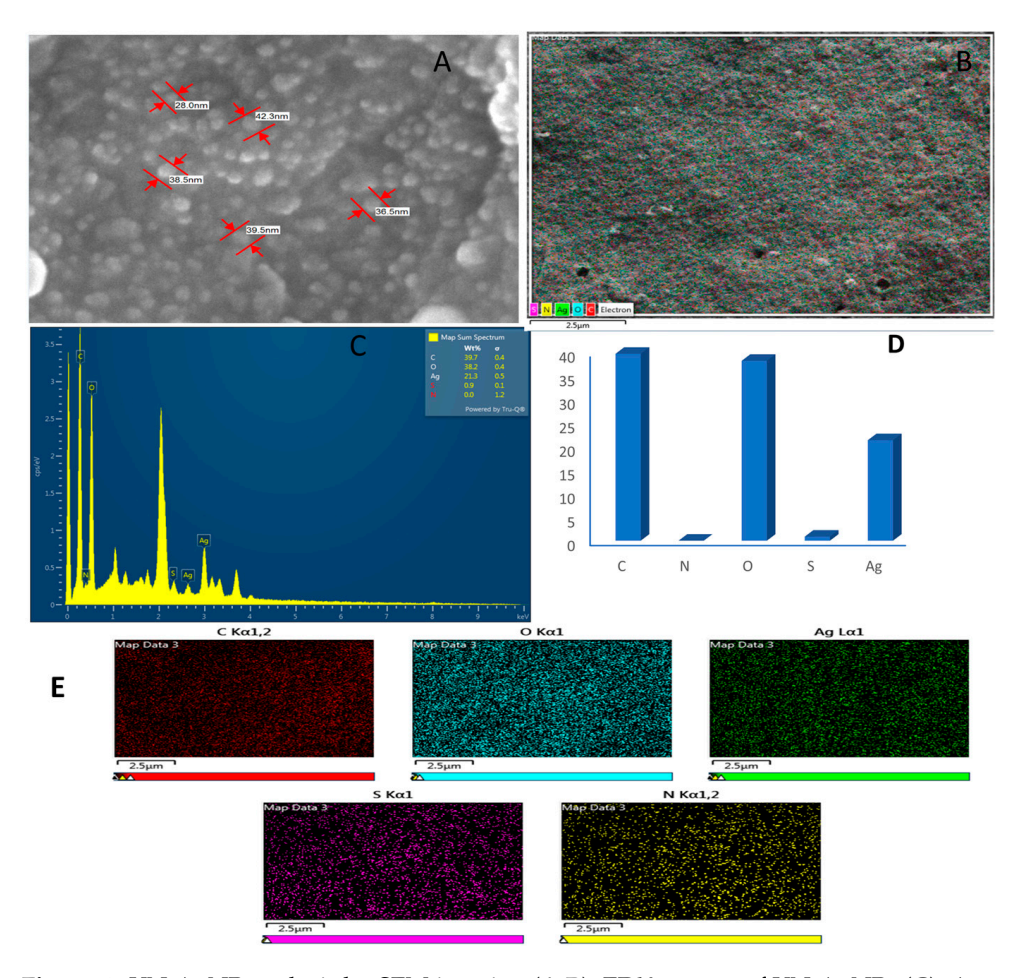


Figure 4. VN-AgNP analysis by SEM imaging (**A**,**B**). EDX spectra of VN-AgNPs (**C**). Amount of element present % wt (**D**). Elemental mapping of C, O, Ag, S, and N (**E**).

The elemental composition of the VN-AgNP surface was also analyzed using EDX, identifying the presence of carbon, nitrogen, sulfur, oxygen, and silver (Figure 4C–E). These elements play a critical role in stabilizing and reducing the synthesized nanoparticles. High carbon (39.65%) and oxygen (38.16%) contents suggest the presence of organic molecules, possibly from a capping agent, stabilizer, or surfactant used in nanoparticle synthesis. Silver accounts for 21.32% by weight but only 3.34% by atomic percentage, indicating that silver is a minor component in terms of atomic count but contributes significantly to the overall weight due to its high atomic mass. The elemental composition supports the successful biosynthesis of AgNPs with organic material (possibly plant-derived) capping or stabilizing the nanoparticles. The Ag content verifies the metallic core, while the C, O, and minor S support biogenic surface modification or functionalization. Ag content (21.3%) is good, but in purely synthesized or metallic AgNPs, this value might be higher (40–70%). However, in green-synthesized or biofunctionalized AgNPs, lower Ag % is normal due to the organic coating. Organic material (C, O) makes these NPs ideal for biomedical or antimicrobial applications, as it reduces toxicity and increases biocompatibility.

Additionally, X-ray diffraction (XRD) analysis was employed to determine the crystallinity of the green-synthesized nanoparticles. The XRD peaks confirmed the crystalline nature of the VN-AgNPs. Variations in the shape and size of the nanoparticles during synthesis were attributed to kinetic factors and molecular rearrangements of atoms. Similar findings were observed in the biosynthesis of silver nanoparticles using *Eucalyptus camaldulensis* and *Terminalia arjuna* extracts [56], as well as in *Aconitum violaceum* [57].

3.4.5. Zeta Potential and DLS

Zeta potential provides insights into the state and long-term stability of nanoparticles in colloidal solutions. The surface electric charge of VN-AgNPs was assessed through zeta potential measurements, which revealed a value of -36.1 mV "Supplementary Materials". The measurement displayed a single peak with a peak area of 100.0% and a standard deviation of 5.97 mV.

The negative zeta potential suggests the potential capping of bio-organic components derived from plant extracts. The strong negative charge indicates that VN-AgNPs are polydispersed in nature, reducing their electrostatic repulsive forces and preventing nanoparticle aggregation. This also confirms the long-term stability of the colloidal solution. The size and diameter of VN-AgNPs in the solution were assessed using DLS analysis. The average particle size and polydispersity index (PDI) of green-produced silver nanoparticles were measured using a nano zeta sizer. The average size of the VN-AgNPs produced was 216 nm "Supplementary Materials". The size obtained is high possibly due to agglomeration in solution, which reduces its efficacy. The nature of produced silver nanoparticles is described by their PDI value; a value more than 0.7 implies polydispersity, while a value less than 0.7 shows the monodispersive nature of nanoparticles [58]. The PDI value of VN-AgNPs was obtained at 0.465, indicating the monodispersed nature of VN-AgNPs. The monodispersive nature shows efficient performance and exceptional use of silver nanoparticles compared to polydispersed nanoparticles.

3.5. Antibacterial and Cytotoxicity Analysis

The antibacterial activity of the synthesized VN-AgNPs was evaluated against four bacterial strains: *Escherichia coli* MTCC443, *Bacillus sphaericus* MTCC7542, *Pseudomonas aeruginosa* MTCC2474, and *Pectobacterium carotovorum* MTCC1428. The activity was assessed by measuring the zones of inhibition. Different concentrations of VN-AgNPs (50 μ L, 70 μ L, 90 μ L, and 110 μ L) were tested to determine their efficacy. The results demonstrated that VN-AgNPs exhibited significant antibacterial activity against all the tested bacterial strains.

The best concentration was 110 µL, at which the diameter of the inhibition zone was 16 ± 0.87 against Bacillus (Gram-positive) and 15 ± 0.46 against E. coli (Gram-negative), 12 ± 0.64 and 11 ± 0.50 against *Pseudomonas* (Gram-negative) and *Pectobacterium* (Gramnegative plant-specific pathogen), respectively (Figure 5). It is shown that tested antibiotic (positive control) and VN-AgNPs generated similar zones of inhibition, which proves the efficacy of nanoparticles against all tested bacteria. The result revealed that the VN-AgNPs worked as an effective antibacterial agent against both Gram-negative and Grampositive strains of tested bacteria. Larger particles might retain bioactive capping molecules from plant extracts or other biomolecules that enhance interaction with bacterial membranes. These bio-organic compounds can exhibit synergistic antibacterial effects with AgNPs. However, for effective antibacterial activity, nanoparticles should ideally be in the 10-200 nm range. Smaller nanoparticles tend to have higher surface-to-volume ratios, which enhances their interaction with bacterial cells, leading to better antibacterial efficacy. Adjusting synthesis and stabilization strategies can improve antibacterial performance. The EDX spectrum confirms that the sample contains silver nanoparticles stabilized by an organic matrix (high C and O). The antibacterial activity is likely dominated by silver (Ag), with possible contributions from sulfur-containing compounds. Further ion release studies and surface analysis will provide deeper insights into the role of silver ions versus nanoparticles in the observed antibacterial effect. Silver nanoparticles show a good inhibitory effect against many bacteria, as proved by similar studies conducted on other plant species green-synthesized silver nanoparticles [59-61].

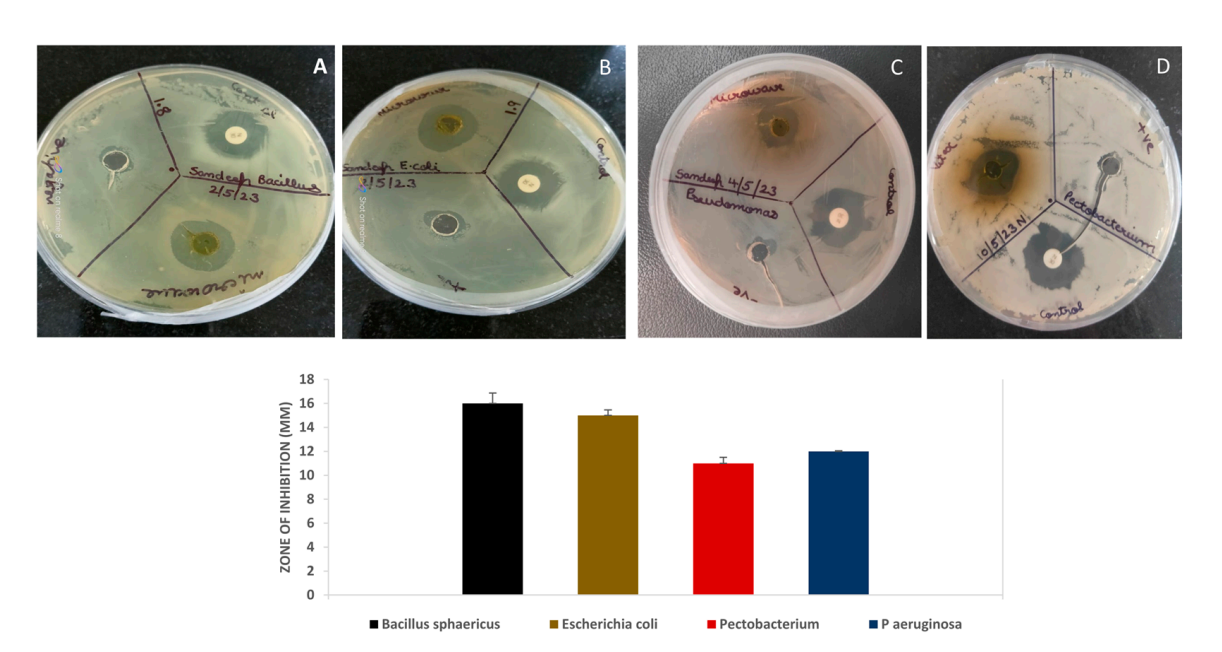


Figure 5. Antibacterial efficacy of VN-AgNPs against "(**A**)": *B. sphaericus*, "(**B**)": *P aeruginosa*, "(**C**)": *E. coli*, and "(**D**)": *P. carotovorum*. The histogram shows the zone of inhibition (Mean \pm SE), n = 3.

3.6. Hemolytic Activity

VN-AgNPs were also evaluated for cytotoxicity using a hemolysis assay, in which various concentrations of VN-AgNPs were tested. For comparison, 1% Triton X-100 and 1X PBS were used as positive and negative controls, respectively (Supp-4). It was observed that VN-AgNPs at a concentration of 20 µg/mL exhibited the lowest hemolytic activity, measuring $1.33 \pm 0.06\%$. As the nanoparticle concentration increased, the percentage of hemolysis also increased (Supp-4). However, even at the highest concentration tested, the hemolysis percentage remained significantly lower compared to the Triton X-100 control. These findings suggest that plant extract-derived silver nanoparticles exhibit minimal toxicity toward RBCs, likely due to the inherently biocompatible nature of plant-derived nanoparticles [62]. Hemolytic assay evaluates the cytotoxicity of plant extract-assisted nanoparticles (NPs), specifically their interaction with red blood cells (RBCs), to determine biocompatibility. This is crucial in developing biomedical applications like drug delivery or antimicrobial therapies. Nanoparticles can attach to or embed within the phospholipid bilayer of RBCs. The surface charge (zeta potential), size, and morphology of nanoparticles influence this interaction. Positively charged or small-sized NPs are more likely to disrupt the membrane, causing leakage of intracellular components like hemoglobin [63]. Some metal-based nanoparticles (e.g., AgNPs, ZnONPs) can generate reactive oxygen species (ROS), leading to oxidative damage of membrane lipids in RBCs, while plant phytochemicalmediated synthesis of nanoparticles may scavenge reactive oxygen species that help to reduce hemolytic activity. It makes green-synthesized nanoparticles more suitable for biomedical applications like drug delivery or antimicrobial therapies [64].

In the present study, phytochemical analysis was conducted using different extraction methods, and their efficiency was compared based on total phenolic content (TPC), total flavonoid content (TFC), and total antioxidant capacity (TAC) data, as these parameters provide valuable insights into the bioactive potential of plant extracts [65,66]. *Vitex negundo* aqueous leaf extract demonstrated promising bioactivity and was therefore selected for the green synthesis of silver nanoparticles (AgNPs). The biosynthesis of AgNPs using plant extracts is highly influenced by physicochemical parameters such as pH, temperature, reaction time, and silver nitrate (AgNO₃) concentration [67]. In this study, the optimized conditions for the green synthesis of silver nanoparticles were identified as 50 °C for 60 min

at pH 9, using a plant extract-to-silver nitrate ratio of 1:2 and an $AgNO_3$ concentration of 4 mM. Under these conditions, a nanoparticle yield of 1.17% was achieved. Optimization of these factors is crucial to ensure the production of nanoparticles with desirable size, shape, and stability for targeted applications. A thorough understanding of these variables facilitates a controlled and reproducible green synthesis process. Furthermore, the synthesized VN-AgNPs were evaluated for their antibacterial activity and hemocompatibility. Despite obtaining silver nanoparticles of relatively larger size post-optimization, the synthesized AgNPs demonstrated strong antibacterial activity, indicating that size is not the sole determinant of antimicrobial efficacy. These findings suggest that other factors—such as surface charge, shape, crystallinity, surface functionalization (e.g., capping agents from plant extracts or other reducing agents), and release of Ag^+ ions—play crucial roles in influencing the antibacterial potential of AgNPs. The results of antibacterial and hemolytic assays confirmed their potential for biomedical applications, highlighting their promise as a safer and more sustainable alternative to chemically synthesized nanoparticles.

4. Conclusions

In conclusion, the study highlights the immense potential of Vitex negundo-mediated biogenic silver nanoparticles as an effective antibacterial agent. These nanoparticles' optimization and structural characterization confirm their successful synthesis. Further studies, such as ICP-MS or AAS, correlation studies, and surface characterization, are required so that the release of Ag⁺ ions from the sample can be measured. This will help confirm whether the antibacterial activity is due to ionic silver or the nanoparticle core. The VN-AgNPs showed good antibacterial efficacy. However, by optimizing the synthesis parameters, we can modify the size of nanoparticles for better results. The findings suggested the growing importance of medicinal plants and their bioactive compounds in pharmaceutical applications, mainly as safer and more effective alternatives to synthetic drugs. Furthermore, this study also provides evidence for integrating nanotechnology with herbal medicine, demonstrating a sustainable and eco-friendly approach to drug development. These results open new ways for further research and development in green nanotechnology and its application in modern therapeutics by offering a novel strategy to address alarming issues such as antibiotic resistance. This work reaffirms the therapeutic potential of natural products and their role in advancing future healthcare solutions.

Supplementary Materials: The following supporting information can be downloaded at: https://www.mdpi.com/article/10.3390/colloids9050055/s1, Figure S1: Graphical representation of the presence frequency of bioactive compounds in Vitex negundo leaf extract in different extraction methods using methanol as solvent; Figure S2: GC–MS profiling of Vitex negundo leaf extract, identified compounds are listed with their structures; Figure S3: (A). Dynamic light scattering (DLS) (B). Zeta potential; Figure S4: Hemolytic activity of methanolic extract of Vitex negundo ((12.5, 25, 50, and $100~\mu g~mL^{-1}$) using different concentration. OD measurements at 576 nm (Y-axis) of blood extract mixture incubated for 30 min at 37 °C with DMSO (-ve control), 10% Triton X-100 (+ve control), Hemolytic activity is represented as the mean \pm standard deviation of 3 replicates and expressed as a percentage of hemolysis; Figure S5 FTIR spectra of Vitex negundo leaf extract; Table S1: Among all tested phytochemicals, saponin were the only one that was absent in the extract.

Author Contributions: All authors contributed significantly to the work and authorized its publication. M.Y.: original draft, conceptualization, data analysis; E.S.: conceptualization and original draft, final editing; N.G.: conceptualization; S.S. and K.K.: data curation and analysis; N.W. final drafting; A.A.: Final Reviewing, Editing and Financial Support. All authors have read and agreed to the published version of the manuscript.

Funding: This research received no external funding.

Data Availability Statement: All data is made available on request.

Acknowledgments: We acknowledge the DST-FIST-sponsored Biotechnology department of School of Biotechnology (SOBT), Gautam Buddha University, for providing the necessary facilities. We also extend our sincere thanks to Gunjan Garg for providing *Vitex negundo* for this research.

Conflicts of Interest: The authors declare that there are no conflicts of interest to declare.

References

1. Khan, F.; Shariq, M.; Asif, M.; Siddiqui, M.A.; Malan, P.; Ahmad, F. Green Nanotechnology: Plant-Mediated Nanoparticle Synthesis and Application. *Nanomaterials* **2022**, *12*, 673. [CrossRef] [PubMed]

- 2. Noah, N.M.; Ndangili, P.M. Green Synthesis of Nanomaterials from Sustainable Materials for Biosensors and Drug Delivery. *Sens. Int.* **2022**, *3*, 100166. [CrossRef]
- 3. Sharma, N.K.; Vishwakarma, J.; Rai, S.; Alomar, T.S.; AlMasoud, N.; Bhattarai, A. Green Route Synthesis and Characterization Techniques of Silver Nanoparticles and Their Biological Adeptness. *ACS Omega* **2022**, *7*, 27004–27020. [CrossRef] [PubMed]
- 4. Sivapalan, S.; Dharmalingam, S.; Ashokkumar, V.; Venkatesan, V.; Angappan, M. Evaluation of the Anti-Inflammatory and Antioxidant Properties and Isolation and Characterization of a New Bioactive Compound, 3,4,9-Trimethyl-7-Propyldecanoic Acid from *Vitex negundo*. *J. Ethnopharmacol.* 2024, 319, 117314. [CrossRef]
- Meena, A.K.; Perumal, A.; Kumar, N.; Singh, R.; Ilavarasan, R.; Srikanth, N.; Dhiman, K.S. Studies on Physicochemical, Phytochemicals, Chromatographic Profiling & Estimation and in-Silico Study of Negundoside in Roots & Small Branches of Vitex negundo Plant. Phytomedicine Plus 2022, 2, 100205. [CrossRef]
- 6. Hano, C.; Abbasi, B.H. Plant-Based Green Synthesis of Nanoparticles: Production, Characterization and Applications. *Biomolecules* **2021**, *12*, 31. [CrossRef]
- 7. Arland, S.E.; Kumar, J. Green and chemical syntheses of silver nanoparticles: Comparative and comprehensive study on characterization, therapeutic potential, and cytotoxicity. *Eur. J. Med. Chem. Rep.* **2024**, *11*, 100168.
- 8. Nasrullah, M.; Gul, F.Z.; Hanif, S.; Mannan, A.; Naz, S.; Ali, J.S.; Zia, M. Green and chemical syntheses of CdO NPs: A comparative study for yield attributes, biological characteristics, and toxicity concerns. *ACS Omega* **2020**, *5*, 5739–5747. [CrossRef]
- 9. Llompart, M.; Garcia-Jares, C.; Celeiro, M.; Dagnac, T. Extraction | Microwave-Assisted Extraction. In *Encyclopedia of Analytical Science*, 3rd ed.; Worsfold, P., Poole, C., Townshend, A., Miró, M., Eds.; Academic Press: Oxford, UK, 2019; pp. 67–77. [CrossRef]
- 10. Bruna, T.; Maldonado-Bravo, F.; Jara, P.; Caro, N. Silver Nanoparticles and Their Antibacterial Applications. *Int. J. Mol. Sci.* **2021**, 22, 7202. [CrossRef]
- 11. Dakal, T.C.; Kumar, A.; Majumdar, R.S.; Yadav, V. Mechanistic Basis of Antimicrobial Actions of Silver Nanoparticles. *Front. Microbiol.* **2016**, *7*, 1831. [CrossRef]
- 12. Santhi, K.; Sengottuvel, R. Qualitative and Quantitative Phytochemical Analysis of *Moringa concanensis* Nimmo. *Int. J. Curr. Microbiol. Appl. Sci.* **2016**, *5*, 633–640. [CrossRef]
- 13. Sivakumar, T. In vitro antioxidant, total phenolic, total flavonoid content and biosynthesis of silver nanoparticles using *Cassia auriculata* leaves extracts. *Int. J. Botany. Stud.* **2021**, *6*, 476–480.
- 14. Silvestrini, A.; Meucci, E.; Ricerca, B.M.; Mancini, A. Total Antioxidant Capacity: Biochemical Aspects and Clinical Significance. *Int. J. Mol. Sci.* **2023**, 24, 10978. [CrossRef] [PubMed]
- 15. Ralte, L.; Khiangte, L.; Thangjam, N.M.; Kumar, A.; Singh, Y.T. GC–MS and Molecular Docking Analyses of Phytochemicals from the Underutilized Plant, *Parkia timoriana* Revealed Candidate Anti-Cancerous and Anti-Inflammatory Agents. *Sci. Rep.* **2022**, 12, 3395. [CrossRef]
- 16. Karimi, S.; Azizi, F.; Nayeb-Aghaee, M.; Mahmoodnia, L. The Antimicrobial Activity of Probiotic Bacteria Escherichia Coli Isolated from Different Natural Sources against Hemorrhagic E. Coli O₁₅₇:H₇. Electron. Physician **2018**, 10, 6548–6553. [CrossRef]
- 17. Aziz, S.B.; Abdullah, O.G.; Saber, D.R.; Rasheed, M.A.; Ahmed, H.M. Investigation of metallic silver nanoparticles through UV-Vis and optical micrograph techniques. *Int. J. Electrochem. Sci.* **2017**, *12*, 363–373. [CrossRef]
- 18. Mughal, T.A.; Ali, S.; Mumtaz, S.; Summer, M.; Saleem, M.Z.; Hassan, A.; Hameed, M.U. Evaluating the biological (antidiabetic) potential of TEM, FTIR, XRD, and UV-spectra observed berberis lyceum conjugated silver nanoparticles. *Microsc. Res. Tech.* **2024**, 87, 1286–1305. [CrossRef]
- 19. Mehta, B.K.; Chhajlani, M.; Shrivastava, B.D. Green synthesis of silver nanoparticles and their characterization by XRD. *J. Phys. Conf. Ser.* **2017**, *836*, 012050. [CrossRef]
- 20. Singh, V.; Shrivastava, A.; Wahi, N. Biosynthesis of silver nanoparticles by plants crude extracts and their characterization using UV, XRD, TEM and EDX. *Afr. J. Biotechnol.* **2015**, *14*, 2554–2567.
- 21. Gontijo, L.A.; Raphael, E.; Ferrari, D.P.; Ferrari, J.L.; Lyon, J.P.; Schiavon, M.A. pH effect on the synthesis of different size silver nanoparticles evaluated by DLS and their size-dependent antimicrobial activity. *Matéria* **2020**, 25, e-12845. [CrossRef]

22. Mandal, M.K.; Domb, A.J. Antimicrobial Activities of Natural Bioactive Polyphenols. *Pharmaceutics* **2024**, *16*, 718. [CrossRef] [PubMed]

- 23. Blomstrand, E.; Posch, E.; Stepulane, A.; Rajasekharan, A.; Andersson, M. Antibacterial and Hemolytic Activity of Antimicrobial Hydrogels Utilizing Immobilized Antimicrobial Peptides. *Int. J. Mol. Sci.* **2024**, *25*, 4200. [CrossRef] [PubMed]
- 24. Gligor, O.; Clichici, S.; Moldovan, R.; Muntean, D.; Vlase, A.-M.; Nadăș, G.C.; Matei, I.A.; Filip, G.A.; Vlase, L.; Crișan, G. The Effect of Extraction Methods on Phytochemicals and Biological Activities of Green Coffee Beans Extracts. *Plants* 2023, 12, 712. [CrossRef] [PubMed]
- 25. Shaikh, J.R.; Patil, M. Qualitative tests for preliminary phytochemical screening: An overview. *Int. J. Chem. Stud.* **2020**, *8*, 603–608. [CrossRef]
- 26. Manso, T.; Lores, M.; de Miguel, T. Antimicrobial Activity of Polyphenols and Natural Polyphenolic Extracts on Clinical Isolates. *Antibiotics* **2021**, *11*, 46. [CrossRef]
- 27. Satchanska, G. Antibacterial Activity of Plant Polyphenols. In *Secondary Metabolites–Trends and Reviews*; IntechOpen: London, UK, 2022. [CrossRef]
- 28. Asbbane, A.; Ibourki, M.; Hallouch, O.; Oubannin, S.; El Boukhari, A.; Bouyahya, A.; Goh, K.W.; Al Abdulmonem, W.; Ait Aabd, N.; Guillaume, D.; et al. A comparative evaluation of the physico-and bio-chemical characteristics and antioxidant activities of six Argan (*Argania spinosa* (L.) Skeels) varieties. *J. Agric. Food Res.* 2025, 19, 101582. [CrossRef]
- 29. Sharma, E.; Gaur, N.; Singh, S.; Mathur, K.; Kumar, K.; Wahi, N.; Garg, G. Extraction optimization of bioactive compounds from *Vitex negundo* through RSM: GC–MS, FTIR, in silico analysis, and antibacterial activity. *J. Plant Biochem. Biotechnol.* 2025. [CrossRef]
- 30. Wang, Y.; Li, X.; Jiang, Q.; Sun, H.; Jiang, J.; Chen, S.; Guan, Z.; Fang, W.; Chen, F. GC-MS analysis of the volatile constituents in the leaves of 14 Compositae plants. *Molecules* **2018**, 23, 166. [CrossRef]
- 31. Kumar, A.; Kaur, S.; Dhiman, S.; Pal Singh, P.; Thakur, S.; Sharma, U.; Kumar, S.; Kaur, S. 1,2-Benzenedicarboxylic Acid, Bis (2-Methyl Propyl) Ester Isolated from *Onosma Bracteata* Wall. Inhibits MG-63 Cells Proliferation via Akt-P53-Cyclin Pathway. *Res. Sq.* 2021. [CrossRef]
- 32. Zhang, H.; Jiang, Z.; Shen, C.; Zou, H.; Zhang, Z.; Wang, K.; Bai, R.; Kang, Y.; Ye, X.-Y.; Xie, T. 5-Hydroxymethylfurfural Alleviates Inflammatory Lung Injury by Inhibiting Endoplasmic Reticulum Stress and NLRP3 Inflammasome Activation. *Front. Cell Dev. Biol.* **2021**, *9*, 782427. [CrossRef]
- 33. Onoja, J. Effects of 5-Hydroxymethylfurfural Isolated from Cola Hispida on Oral Adenosquamous Carcinoma and MDR Staphylococcus Aureus. *J. Med. Plant Herb. Ther. Res.* **2021**, *8*, 1–7.
- 34. Ochieng Nyalo, P.; Isanda Omwenga, G.; Piero Ngugi, M. GC-MS Analysis, Antibacterial and Antioxidant Potential of Ethyl Acetate Leaf Extract of Senna Singueana (Delile) Grown in Kenya. *Evid. Based Complement. Altern. Med.* 2022, 2022, 5436476. [CrossRef] [PubMed]
- 35. Hassane, A.M.A.; Hussien, S.M.; Abouelela, M.E.; Taha, T.M.; Awad, M.F.; Mohamed, H.; Hassan, M.M.; Hassan, M.H.A.; Abo-Dahab, N.F.; El-Shanawany, A.-R.A. In Vitro and In Silico Antioxidant Efficiency of Bio-Potent Secondary Metabolites From Different Taxa of Black Seed-Producing Plants and Their Derived Mycoendophytes. Front. Bioeng. Biotechnol. 2022, 10, 930161. [CrossRef] [PubMed]
- 36. Lee, H.Y.; Back, K. The Antioxidant Cyclic 3-Hydroxymelatonin Promotes the Growth and Flowering of Arabidopsis Thaliana. *Antioxidants* **2022**, *11*, 1157. [CrossRef]
- 37. Lomelí-Rosales, D.A.; Zamudio-Ojeda, A.; Reyes-Maldonado, O.K.; López-Reyes, M.E.; Basulto-Padilla, G.C.; Lopez-Naranjo, E.J.; Zuñiga-Mayo, V.M.; Velázquez-Juárez, G. Green Synthesis of Gold and Silver Nanoparticles Using Leaf Extract of Capsicum Chinense Plant. *Molecules* 2022, 27, 1692. [CrossRef]
- 38. Malik, M.; Iqbal, M.A.; Malik, M.; Raza, M.A.; Shahid, W.; Choi, J.R.; Pham, P.V. Biosynthesis and Characterizations of Silver Nanoparticles from Annona Squamosa Leaf and Fruit Extracts for Size-Dependent Biomedical Applications. *Nanomaterials* **2022**, 12, 616. [CrossRef]
- 39. Ajaykumar, A.P.; Mathew, A.; Chandni, A.P.; Varma, S.R.; Jayaraj, K.N.; Sabira, O.; Rasheed, V.A.; Binitha, V.S.; Swaminathan, T.R.; Basheer, V.S.; et al. Green Synthesis of Silver Nanoparticles Using the Leaf Extract of the Medicinal Plant, Uvaria Narum and Its Antibacterial, Antiangiogenic, Anticancer and Catalytic Properties. *Antibiotics* 2023, 12, 564. [CrossRef]
- 40. Giri, A.K.; Jena, B.; Biswal, B.; Pradhan, A.K.; Arakha, M.; Acharya, S.; Acharya, L. Green Synthesis and Characterization of Silver Nanoparticles Using Eugenia Roxburghii DC. Extr. Act. Against Biofilm-Prod. Bacteria. Sci. Rep. 2022, 12, 8383. [CrossRef]
- 41. Sundar, M.; Rajagopal, G.; Nivetha, A.; Prabu Kumar, S.; Muthukumar, S. Phyto-Mediated Green Synthesis of Silver Nanoparticles Using an Aqueous Leaf Extract of Momordica Cymbalaria: Antioxidant, Cytotoxic, Antibacterial, and Photocatalytic Properties. Separations 2024, 11, 61. [CrossRef]
- 42. Liu, H.; Zhang, H.; Wang, J.; Wei, J. Effect of Temperature on the Size of Biosynthesized Silver Nanoparticle: Deep Insight into Microscopic Kinetics Analysis. *Arab. J. Chem.* **2020**, *13*, 1011–1019. [CrossRef]

43. Ansari, M.; Ahmed, S.; Abbasi, A.; Khan, M.T.; Subhan, M.; Bukhari, N.A.; Hatamleh, A.A.; Abdelsalam, N.R. Plant mediated fabrication of silver nanoparticles, process optimization, and impact on tomato plant. *Sci. Rep.* **2023**, *13*, 18048. [CrossRef] [PubMed]

- 44. Muhammad, R.; Mutreja, V.; Sareen, S.; Ahmad, B.; Faheem, M.; Zahid, N.; Jabbour, G.; Park, J. Exceptional antibacterial and cytotoxic potency of monodisperse greener AgNPs prepared under optimized pH and temperature. *Sci. Rep.* **2021**, *11*, 2866.
- 45. Molleman, B.; Hiemstra, T. Time, pH, and size dependency of silver nanoparticle dissolution: The road to equilibrium. *Environ. Sci. Nano* **2017**, *4*, 1314–1327. [CrossRef]
- 46. Fernando, I.; Zhou, Y. Impact of pH on the stability, dissolution and aggregation kinetics of silver nanoparticles. *Chemosphere* **2019**, *216*, 297–305. [CrossRef]
- 47. Bergal, A.; Matar, G.H.; Andaç, M. Olive and Green Tea Leaf Extracts Mediated Green Synthesis of Silver Nanoparticles (AgNPs): Comparison Investigation on Characterizations and Antibacterial Activity. *BioNanoScience* 2022, 12, 307–321. [CrossRef]
- 48. Ghoshal, G.; Singh, M. Characterization of silver nano-particles synthesized using fenugreek leave extract and its antibacterial activity. *Mater. Sci. Energy Technol.* **2022**, *5*, 22–29. [CrossRef]
- 49. Restrepo, C.V.; Villa, C.C. Synthesis of silver nanoparticles, influence of capping agents, and dependence on size and shape: A review. *Environ. Nanotechnol. Monit. Manag.* **2021**, *15*, 100428. [CrossRef]
- 50. Singh, S.; Bharti, A.; Meena, V.K. Green Synthesis of Multi-Shaped Silver Nanoparticles: Optical, Morphological and Antibacterial Properties. *J. Mater. Sci. Mater. Electron.* **2015**, *26*, 3638–3648. [CrossRef]
- 51. Miranda, A.; Akpobolokemi, T.; Chung, E.; Ren, G.; Raimi-Abraham, B.T. pH alteration in plant-mediated green synthesis and its resultant impact on antimicrobial properties of silver nanoparticles (AgNPs). *Antibiotics* **2022**, *11*, 1592. [CrossRef]
- 52. Dash, B.; Mishra, R.K.; Panda, S.K. In-vitro antioxidant activity, pharmacognostical evaluation, HPTLC and FTIR fingerprinting of Phyllanthus acidus L. stem bark extract. *Biomed. Pharmacol. J.* **2023**, *16*, 1575–1583.
- 53. Ogbe, R.J.; Ojighenvo, A.J.; Nwajiaku, L.O.; Audu, O.C.; Ibeji, C.U. FTIR analysis of the phytochemical components of Urtica dioica L. (Urticaceae) whole plant. *J. Pharmacogn. Phytother.* **2021**, *13*, 30–35.
- 54. Ali, M.H.; Azad, M.A.K.; Khan, K.A.; Rahman, M.O.; Chakma, U.; Kumer, A. Analysis of Crystallographic Structures and Properties of Silver Nanoparticles Synthesized Using PKL Extract and Nanoscale Characterization Techniques. *ACS Omega* 2023, 8, 28133–28142. [CrossRef] [PubMed]
- 55. Zulfiqar, Z.; Khan, R.R.; Summer, M.; Saeed, Z.; Pervaiz, M.; Rasheed, S.; Shehzad, B.; Kabir, F.; Ishaq, S. Plant-mediated green synthesis of silver nanoparticles: Synthesis, characterization, biological applications, and toxicological considerations: A review. *Biocatal. Agric. Biotechnol.* **2024**, *19*, 103121. [CrossRef]
- 56. Alghoraibi, I.; Soukkarieh, C.; Zein, R.; Alahmad, A.; Walter, J.G.; Daghestani, M. Aqueous extract of Eucalyptus camaldulensis leaves as reducing and capping agent in biosynthesis of silver nanoparticles. *Inorg. Nano-Met. Chem.* **2020**, *50*, 895–902. [CrossRef]
- 57. Ahmad, S.; Ahmad, S.; Xu, Q.; Khan, I.; Cao, X.; Yang, R.; Yan, H. Green Synthesis of Gold and Silver Nanoparticles Using Crude Extract of Aconitum Violaceum and Evaluation of Their Antibacterial, Antioxidant and Photocatalytic Activities. *Front. Bioeng. Biotechnol.* **2024**, *11*, 1320739. [CrossRef]
- 58. Mazzonello, A.; Valdramidis, V.V.; Farrugia, C.; Grima, J.N.; Gatt, R. Synthesis and characterization of silver nanoparticles. *Int. J. Morden Eng. Res.* **2017**, *7*, 41–47.
- 59. Fareed, N.; Nisa, S.; Bibi, Y.; Fareed, A.; Ahmed, W.; Sabir, M.; Alam, S.; Sajjad, A.; Kumar, S.; Hussain, M.; et al. Green Synthesized Silver Nanoparticles Using Carrot Extract Exhibited Strong Antibacterial Activity against Multidrug Resistant Bacteria. *J. King Saud. Univ.—Sci.* 2023, 35, 102477. [CrossRef]
- 60. Hamad, A.; Khashan, K.S.; Hadi, A. Silver nanoparticles and silver ions as potential antibacterial agents. *J. Inorg. Organomet. Polym. Mater.* **2020**, *30*, 4811–4828. [CrossRef]
- 61. Urnukhsaikhan, E.; Bold, B.-E.; Gunbileg, A.; Sukhbaatar, N.; Mishig-Ochir, T. Antibacterial Activity and Characteristics of Silver Nanoparticles Biosynthesized from Carduus Crispus. *Sci. Rep.* **2021**, *11*, 21047. [CrossRef]
- 62. Nelsonjoseph, L.; Vishnupriya, B.; Amsaveni, R.; Bharathi, D.; Thangabalu, S.; Rehna, P. Synthesis and characterization of silver nanoparticles using Acremonium borodinense and their anti-bacterial and hemolytic activity. *Biocatal. Agric. Biotechnol.* **2022**, 39, 102222. [CrossRef]
- 63. Bhattacharjee, S. DLS and zeta potential—what they are and what they are not? *J. Control. Release* **2016**, 235, 337–351. [CrossRef] [PubMed]
- 64. Kumar, K.V.; Varadaraju, K.R.; Shivaramu, P.D.; Kumar, C.H.; Prakruthi, H.R.; Shekara, B.C.; Shreevatsa, B.; Wani, T.A.; Prakasha, K.C.; Kollur, S.P.; et al. Bactericidal, anti-hemolytic, and anticancerous activities of phytofabricated silver nanoparticles of glycine max seeds. Front. Chem. 2024, 12, 1427797. [CrossRef] [PubMed]
- 65. Phuyal, N.; Jha, P.K.; Raturi, P.P.; Rajbhandary, S. Total phenolic, flavonoid contents, and antioxidant activities of fruit, seed, and bark extracts of Zanthoxylum armatum DC. *Sci. World J.* **2020**, 2020, 8780704. [CrossRef] [PubMed]

66. Ezealigo, U.S.; Joshua, P.E.; Ononiwu, C.P.; Agbo, M.O.; Asomadu, R.O.; Ogugua, V.N. Total phenolic and flavonoid content and in vitro antioxidant activity of methanol extract and solvent fractions of *Desmodium ramosissimum* G. Don. *Med. Sci. Forum* **2021**, 2, 15.

67. Bala, A.; Rani, G. A review on phytosynthesis, affecting factors and characterization techniques of silver nanoparticles designed by green approach. *Int. Nano Lett.* **2020**, *10*, 159–176. [CrossRef]

Disclaimer/Publisher's Note: The statements, opinions and data contained in all publications are solely those of the individual author(s) and contributor(s) and not of MDPI and/or the editor(s). MDPI and/or the editor(s) disclaim responsibility for any injury to people or property resulting from any ideas, methods, instructions or products referred to in the content.